X-ray Emission Line Profile Modeling of O stars: ζ Puppis as a Wind-Shock Source

Roban H. Kramer[1], **David H. Cohen**[1], **Stanley P. Owocki**[2]

[1] *Swarthmore College Dept. of Physics and Astronomy;* [2] *Bartol Research Institute, University of Delaware*

Hot-star winds

- Massive (up to 60 $M_\odot$), hot ($T_{\rm eff} \sim 10^4$ K) stars are extremely luminous (up to $10^6 L_\odot$).
- Their intense radiation drives massive winds (up to $\dot{M} \sim 10^{-5}\,{\rm M_\odot yr^{-1}}$) which reach velocities of a few 1000 km s^{-1}.
- The *Chandra* and *XMM* x-ray observatories detect strong x-ray emission from such stars in spectral lines of highly ionized heavy atoms (primarily H-like and He-like lines of N, O, Ne, Mg, Al, Si, and S, and L-shell lines of Fe).
- The mechanism responsible for heating gas to the temperatures needed to produce such ionization states is a mystery, but leading theories suggest **shocks distributed throughout the wind**. Each shock model, however, predicts different physical properties for the shocked wind.

A spherically-symmetric, parametrized model

We adopt the flexible line profile model developed by Owocki & Cohen (2001), who make the following key assumptions:

1. The wind is spherically-symmetric and time-independent.
2. The hot, shocked component of the wind emits x-rays which are Doppler shifted by high wind velocities. The cold, unshocked component of the wind absorbs x-rays passing through it. These components are uniformly mixed throughout the wind (though the hot component only exists above a certain radius, see assumption 4).
3. The velocity of the wind is given by
$$v(r) = v_\infty \left(1 - R_*/r\right)^\beta . \qquad (1)$$
4. Above some minimum radius $R_{\rm o}$, the emissivity is proportional to density squared, with an extra factor of r^{-q}. Below $R_{\rm o}$ there is no emission. The emission occurs at a single rest wavelength (natural, thermal, and turbulent broadening are neglected).
5. An optical depth is assigned to each point in the wind by integrating along the observer's line of sight. For lines of sight not intersecting the opaque star
$$\tau(\mu, r) = \tau_* \int_{\mu r}^{\infty} \frac{R_* dz'}{r'^2 (1 - R_*/r')^\beta} \text{ with } r' \equiv \sqrt{p^2 + z'^2} \qquad (2)$$

Combining these assumptions, the line profile, parameterized by the four values β, q, $R_{\rm o}$, and τ_*, is given by

$$L_\lambda \propto \int_{r=R_{\rm o}}^{\infty} \frac{r^{-(q+2)}}{(1 - R_*/r)^{2\beta}} \exp\left[-\tau\left(\frac{x}{(1 - R_*/r)^\beta}, r\right)\right] dr \, . \qquad (3)$$

We integrate this equation numerically to obtain line profiles. Before comparing a profile with an observed spectrum it is convolved with an instrumental response function, binned to match the data, and normalized to the observed flux. It is convenient to plot line profiles as functions of a scaled wavelength coordinate,

$$x \equiv \frac{\Delta\lambda/\lambda_0}{v_\infty/c} \, . \qquad (4)$$

Line transport in an expanding medium with continuum absorption

Emission

Below we build up **a wind and emission line profile** (in the absence of absorption) by adding up thin, expanding, spherical shells. Doppler shifting of the expanding wind broadens lines. The observer looks at the star from the left. The "front" (left) side of the wind will appear blueshifted while the "back" (right) is redshifted. Each shell produces a flat-topped profile with its width set by the shell velocity.

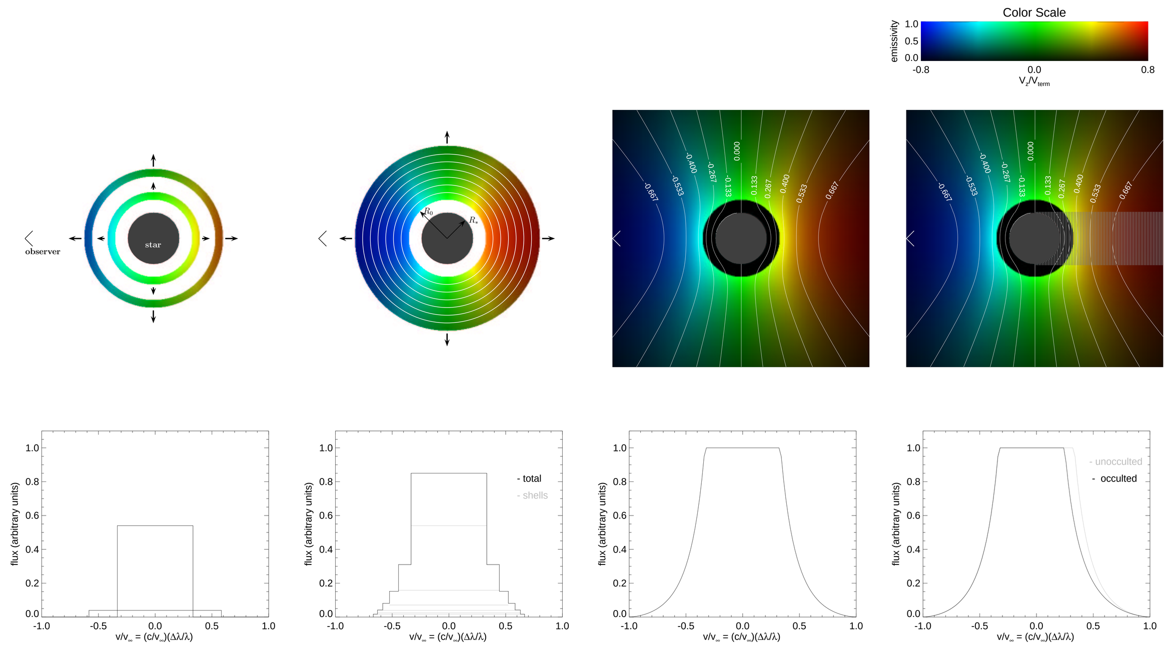

Inner shells are slower and more dense, producing narrower, taller line profiles.

A series of shells, added together, produce a stepped profile.

A continuous wind is built by integrating shells from some minimum radius to infinity.

Occultation by the star removes light from the red edge of the profile.

Wind maps and line profiles: In the maps, **hue** is used to indicate the **line-of-sight component of wind velocity** (for the observer to the left of the star), and **brightness** indicates **x-ray volume emissivity**. Under each map is the corresponding line profile with the bluest wavelengths (expressed in velocity units) on the left, and the reddest on the right.

Continuum absorption

Including continuum absorption by the cold component of the wind preferentially removes red photons, which arise at higher optical depths.

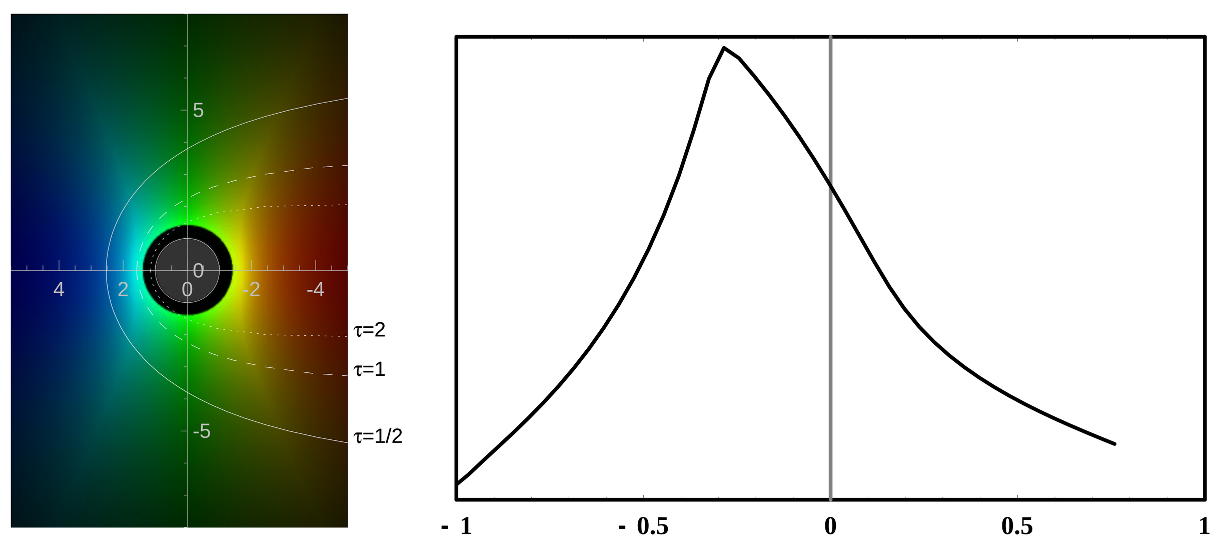

Contours of constant optical depth (integrated along the observer's line of sight) overlaying a **velocity color map** (left) and the resulting **line profile** (right) show the effect of an optically thick wind.

A flexible model

This model can parameterize many different types of wind x-ray distributions, allowing for the testing of different physical theories.

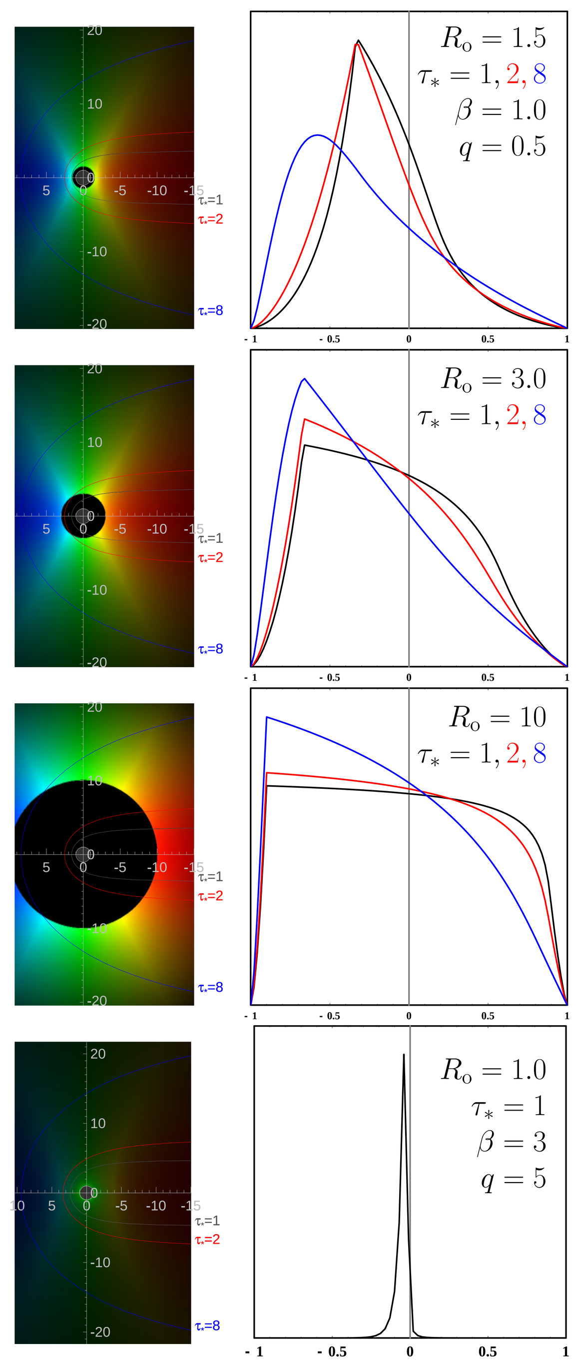

Contours of optical depth unity overlaying **color velocity maps** (far left) with corresponding **line profiles** (immediate left) for different values of τ_*.

Varying the minimum radius of x-ray emission ($R_{\rm o}$) and the intrinsic optical depth of the wind (τ_*) affects the shape of the profiles. Larger minimum radii exclude inner, slow-moving regions of the wind, resulting in broader, flatter profiles. Higher intrinsic optical depths obscure reddened regions, skewing the line blueward.

To mimic a **coronal** model of x-ray production we let the emissivity drop off like a high power of $1/r$, producing narrow profiles (left).

Three-parameter fits to high-resolution spectra

We fit the model to eight lines between 6.18 Å (Si XIV) and 24.78 Å (N VII) in the *Chandra* spectrum of the O4 supergiant ζ Puppis. This star has a luminosity of $10^6 L_\odot$ and a surface temperature of 42000 K (seven times solar).

Below we show **the fit to the 15.013 Å line of Fe XVII** from the *Chandra* spectrum of ζ Puppis. The data are show as diamonds with error bars, the solid line is the model (convolved, binned and normalized).

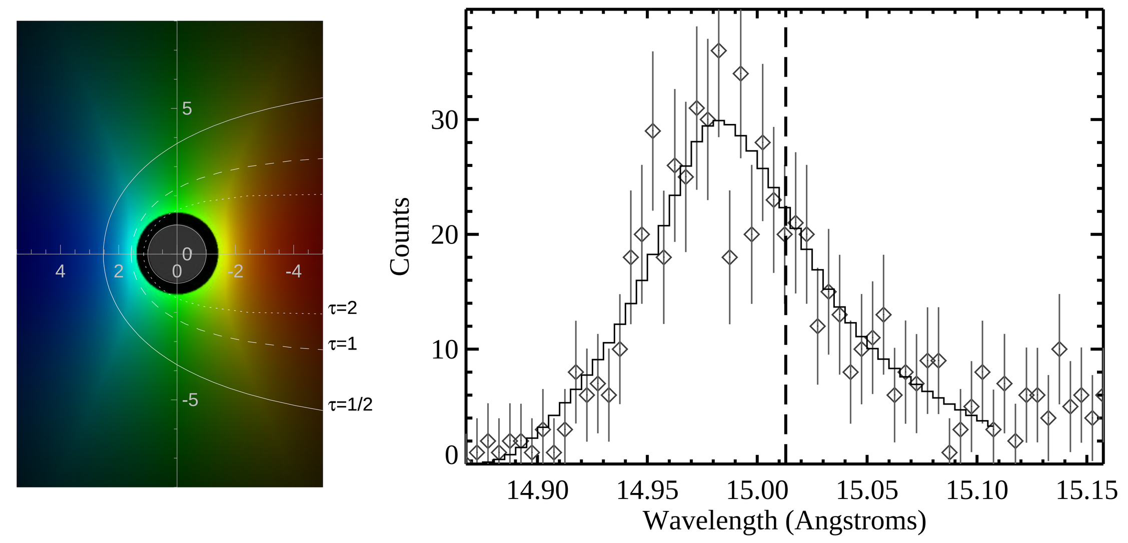

The fit parameters are

$$\beta = 1 \text{ (fixed)}, \; q = -0.2, \; R_{\rm o} = 1.4 \text{ and, } \tau_* = 1.0 \, .$$

Results for the *Chandra* spectrum of ζ Puppis

Best-fit and extreme models for the O XVIII line at 18.97 Å are shown demonstrating the range of models that can be fit to a single line. Shown are the fit with τ_* held at its 95.4% confidence upper limit ($\tau_* = 5.0$; line profile green, left wind map), best fit ($\tau_* = 2.5$; line profile black, center wind map) and fit with τ_* held at its 95.4% confidence lower limit ($\tau_* = 1.0$; line profile in purple, right wind map).

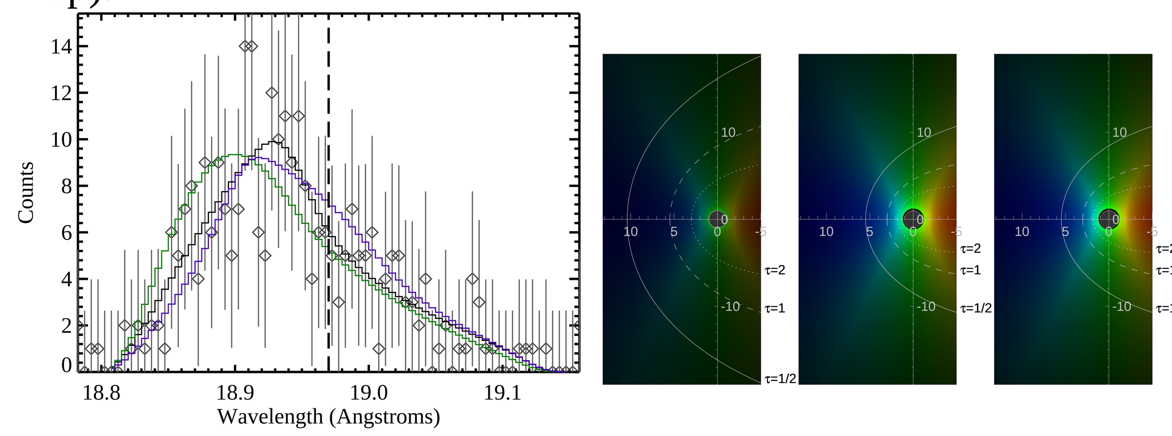

Model parameters versus wavelength (best-fit values and 95.4% confidence limits) for seven analyzed lines (to appear in Kramer, Cohen, & Owocki, 2003). All fits were performed with a fixed value of $\beta = 1$.

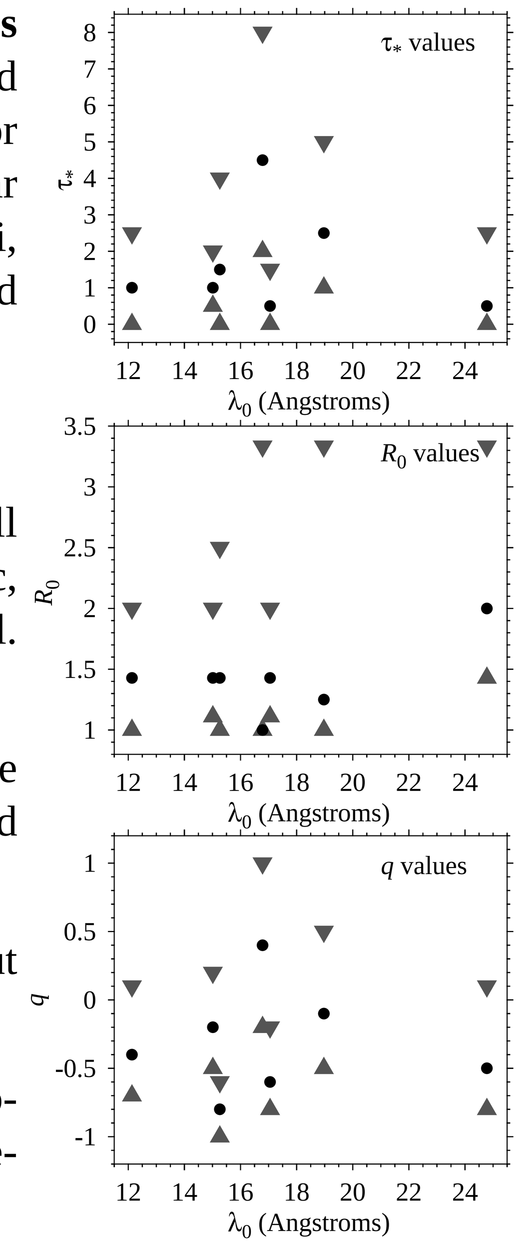

Key conclusions:

1. ζ Puppis line profiles are well fit by a spherically-symmetric, distributed-wind-shock model.
2. X-ray emission begins near the surface of the star (indicated by small $R_{\rm o}$ values).
3. Wind x-ray opacity is low but non-zero.
4. Fit parameters exhibit no obvious trends with line wavelength.

Conclusion 3 is surprising because significantly higher values of τ_* were expected, given prior determinations of the star's mass-loss rate. This may be indicative of clumping, which could reduce the effective opacity of the wind. We were also intrigued to find little variation in τ_* with wavelength. This is surprising because photoionization cross sections should scale roughly as λ^3. This could be an effect of the distribution of ionization edges, or, perhaps, extreme clumping.

See also

Kramer, R. H., Cohen, D. H., & Owocki, S. P. 2003, Astrophys. J. Letters, submitted, `http://arxiv.org/abs/astro-ph/0211550`

Owocki, S. P. & Cohen, D. H. 2001, Astrophys. J., 559, 1108

For an electronic version of this poster, paper preprints, and updates, visit `http://www.sccs.swarthmore.edu/~roban/x-ray/` or `http://astro.swarthmore.edu/~cohen/`